Structural and Thermal Properties of $La_{1-x}Sr_xCoO_{3-\delta}$

Johann Mastin, Mari-Ann Einarsrud, and Tor Grande*

Department of Materials Science and Engineering, Norwegian University of Science and Technology, 7491 Trondheim, Norway

Received July 4, 2006. Revised Manuscript Received September 22, 2006

The crystal structure and the thermal properties of $La_{1-x}Sr_xCoO_{3-\delta}$ ($0 \leq x \leq 0.5$) perovskites have been investigated by high-temperature X-ray diffraction. At ambient temperature, the crystal structure changes from a rhombohedral structure with the space group $R\bar{3}c$ to a cubic structure with space group $Pm\bar{3}m$ at $x \geq 0.55$. The thermal evolution of the lattice parameters was determined by Rietveld refinement of the diffraction data. The rhombohedral distortion from cubic symmetry decreased nearly linearly with increasing temperature up to the phase transition to the cubic perovskite structure. The linear thermal expansion coefficients of the lattice parameters were found and the rhombohedral to cubic phase transition temperature was determined. The phase transition temperature decreases rapidly with increasing Sr content in $La_{1-x}Sr_xCoO_{3-\delta}$. The phase transition is discussed with relation to the angle of rotation and the strain parameter of the CoO_6 octahedra. Finally, the structural and thermal properties of Sr- and Ca-substituted $LaCoO_3$ are compared, demonstrating the significant difference in the effect of the two alkaline earth cations.

Introduction

$La_{1-x}A_xCoO_3$ with $A = Sr^{2+}$ or Ca^{2+} crystallizes in the perovskite ABO_3 structure with the ideal cubic $Pm\bar{3}m$ space group at elevated temperatures. $LaCoO_3$ undergoes a displacive phase transition at a critical temperature, T_c, and transforms to a rhombohedrally distorted cubic structure with the $R\bar{3}c$ space group at low temperature.[1] With substitution of La^{3+} by Sr^{2+}or Ca^{2+}, the phase transition temperature, T_c, is lowered from about 1340 °C for $LaCoO_3$ [1] to ambient temperature for ∼50 mol % Ca^{2+} [2,3] and ∼55 mol % Sr^{2+}.[4] Substitution of La^{3+} with Sr^{2+} or Ca^{2+} is compensated by a mixed valence of Co (Co^{3+}/Co^{4+}) and/or by creation of oxygen vacancies at high Sr or Ca substitution level. At high temperature, thermal reduction of Co introduces chemical expansion in $La_{1-x}A_xCoO_{3-\delta}$.[5,6] At high substitution level the oxidation of the materials during cooling becomes sluggish, resulting in an apparent constant oxygen defect concentration at low temperature.

The deviation from cubic symmetry is caused by rotation and compression of the CoO_6 octahedra along one of the four diagonals in the cubic unit cell.[7] In the rhombohedral symmetry, the compressed pseudo cubic [111] direction becomes equal to the hexagonal *c*-axis, giving four possible equivalent domain states. These domains meet on the pseudocubic (100) and (110) planes to form (100) and (110) twins.[8,9] Twins in $LaCoO_3$-based materials have been confirmed by electron microscopy.[10] Under external stress, the domains having the compressed body diagonal close to the stress direction will have lower free energy and grow at the expense of the less energetically favorable domain orientations. Domain reorientation during uniaxial compression has been confirmed by synchrotron X-ray diffraction.[11]

The reorientation of ferroelastic domains as a response to mechanical stress is the microscopic origin of ferroelastic behavior of $LaCoO_3$-based materials. Ferroelastic materials are characterized by a ferroelastic hysteresis defined by the cohersive stress and spontaneous strain.[12] Kleveland et al.[13] and Faaland et al.[14] have shown that $LaCoO_3$-based materials display nonlinear behavior under mechanical compression and a remnant strain after unloading. Domain reorientation under mechanical stress in ferroelastic materials opens up for mechanical toughening of the materials. During propagation of a crack, domain switching will absorb energy and,

* Corresponding author. E-mail: Tor.Grande@material.ntnu.no.

(1) Kobayashi, Y.; Mitsunaga, T.; Fujinawa, G.; Arii, T.; Suetake, M.; Asai, K.; Harada, J. *J. Phys. Soc. Jpn.* **2000**, *69* (10), 3468−3469.
(2) Mastin, J.; Einarsrud, M.-A.; Grande, T. *Chem. Mater.* **2006**, *18* (6), 1680−1687.
(3) Faaland, S.; Einarsrud, M.-A.; Grande, T. *Chem. Mater.* **2001**, *13* (3), 723−732.
(4) Mineshige, A.; Inaba, M.; Yao, T. S.; Ogumi, Z.; Kikuchi, K.; Kawase, M. *J. Solid State Chem.* **1996**, *121* (2), 423−429.
(5) Chen, X. Y.; Yu, J. S.; Adler, S. B. *Chem. Mater.* **2005**, *17* (17), 4537−4546.
(6) Lein, H. L.; Wiik, K.; Grande, T. *Solid State Ionics* **2006**, *177*, 1795−1798.
(7) Thornton, G.; Tofield, B. C.; Hewat, A. W. *J. Solid State Chem.* **1986**, *61* (3), 301−307.
(8) Kim, C. H.; Jang, J. W.; Cho, S. Y.; Kim, I. T.; Hong, K. S. *Physica B* **1999**, *262* (3−4), 438−443.
(9) Kim, C. H.; Cho, S. Y.; Kim, I. T.; Cho, W. J.; Hong, K. S. *Mater. Res. Bull.* **2001**, *36* (9), 1561−1571.
(10) Walmsley, J. C.; Bardal, A.; Kleveland, K.; Einarsrud, M.-A.; Grande, T. *J Mater. Sci.* **2000**, *35*, 4251−4260.
(11) Vullum, P. E.; Mastin, J.; Wright, J.; Einarsrud, M.-A.; Holmestad, R.; Grande, T. *Acta Mater.* **2006**, *54*, 2615−2624.
(12) Salje, E. K. H. *Phase transitions in ferroelastic and co-elastic crystals*; Cambridge University Press: Cambridge, 1990.
(13) Kleveland, K.; Orlovskaya, N.; Grande, T.; Moe, A. M. M.; Einarsrud, M.-A.; Breder, K.; Gogotsi, G. *J. Am. Ceram. Soc.* **2001**, *84* (9), 2029−2033.
(14) Faaland, S.; Grande, T.; Einarsrud, M.-A.; Vullum, P. E.; Holmestad, R. *J. Am. Ceram. Soc.* **2005**, *88* (3), 726−730.

10.1021/cm061539k CCC: $33.50
Published on Web 11/07/2006

hence, reduce the crack growth velocity. The mechanical properties of these materials are therefore dependent on the crystal structure and can hence be tailored through controlling the rhombohedral to cubic phase transition temperature via chemical substitution.

The structure of $La_{1-x}Sr_xCoO_{3-\delta}$ at ambient temperature has been reported by several authors,[4,6,15−18] while the thermal evolution of the crystal structure of Sr-substituted $LaCoO_3$ has not been reported so far. Here we report the structural and thermal properties of $La_{1-x}Sr_xCoO_{3-\delta}$ with the aim to investigate the rhombohedral to cubic phase transition. The influence of the alkaline earth cation on the structural and thermal properties is addressed by comparing the present findings with a recent report on $La_{1-x}Ca_xCoO_{3-\delta}$.[2] Finally, the order parameter of the phase transition is discussed with relation to ferroelastic properties.

Experimental Section

$La_{1-x}Sr_xCoO_{3-\delta}$ ($x = 0$, 0.1, 0.2) powders were prepared by solid-state reaction between La_2O_3 (Fluka, >99.98%), Co_3O_4 (Fluka, >99.995%), and $SrCO_3$ (BDH, min. 98.5%). Dried starting materials were mixed together by ball milling in ethanol for 24 h using Si_3N_4 balls and pressed into pellets which were fired twice at 1200 °C for 20 h ($x = 0$) and 6 h ($x = 0.1$ and 0.2) with intermediate grindings. In addition, powders of $La_{1-x}Sr_xCoO_{3-\delta}$ with $x = 0.3$, 0.4, and 0.5 were prepared by spray pyrolysis of metal nitrate solutions made from $Sr(NO_3)_2$ (Merck min. 99%), $Co(NO_3)_2{\cdot}6H_2O$ (Fluka, min. 98.0%), and $La(NO_3)_3{\cdot}6H_2O$) (Merck, min. 99.0%). These powders were prepared for a different purpose but were convenient to use also for the present purpose. Thermogravimetric analyses of the solutions were performed to ensure the correct stoichiometry. See Wiik et al.[19] for a detailed overview of the synthesis by spray pyrolysis. The as-synthesized powders were ball-milled in ethanol for 24 h using Si_3N_4 balls and heat-treated for 6 h at 1200 °C to coarsen the grains. Before analysis, the powders were annealed at 700 °C for 24 h in air to oxidize the materials to obtain close to the stoichiometric oxygen content. All the powders were single-phase materials according to X-ray diffraction.

The oxygen nonstoichiometry of some of the materials was measured. The powder (~300 mg) was heated in a reducing atmosphere (5% H_2/N_2) at 1300 °C for 24 h. The weight loss during the annealing was used to determine the oxygen content based on reaction (1) confirmed by X-ray diffraction.

$$La_{1-x}Sr_xCoO_{3-\delta}(s) \rightarrow \frac{(1-x)}{2}La_2O_3(s) + xSrO(s) + Co(s) + \left[\frac{(3-\delta)+(x-3)/2}{2}\right]O_2(g) \quad (1)$$

X-ray diffraction (XRD) at ambient temperature was performed with a Siemens D5005 $2\theta-\theta$ diffractometer using Cu Kα radiation and a primary monochromator (2θ range 20−110°). The annealed powders were studied by high-temperature XRD (HTXRD) using Siemens D5005 $\theta-\theta$ diffractometer with Cu Kα radiation and a secondary monochromator (2θ range 20−90°). The powders were dispersed in ethanol (100%) and applied on a platinum strip located in a high-temperature camera (HTK 16, Anton Paar GMbh). The measurements were performed in flowing synthetic air (99.99%). Prior to each scan, the powders were held for 30 min at the temperature to establish equilibrium. The data were collected with a step size of 0.03° and a count time of 5−10 s to obtain a good signal-to-noise ratio.

The unit-cell parameters were refined by the Rietveld method[20] using the program TOPAS R (Bruker AXS, version 2.1). The background was refined using a fourth-order Chebichev function. A Pearson VII function was used to refine the peak shape of both Pt and the material under investigation. Reflections due to Pt were refined using the cubic space group $Fm\bar{3}m$. Lattice expansion of Pt was in good agreement with the literature.[21] For the perovskites the cubic $Pm\bar{3}m$ or $R\bar{3}c$ space group were used. The crystal structure parameters and peak shape were finally refined simultaneously with zero point and scale. The oxygen position was also refined for the $R\bar{3}c$ despite the relative large uncertainty in the resulting position. The atomic positions for the space group are (0, 0, 1/4) for La^{3+}/Sr^{2+}, (0, 0, 0) for Co^{3+}, and (x, 0, 1/4) for O^{2-} with $x = 1/2 + u$ where u is the displacement from the ideal cubic position. Below 500 °C, refinement of the isotropic temperature factor β gave inconsistency with temperature, but this parameter had no significant influence on the refined oxygen positions. Therefore, β was fixed to 0.5 for La^{3+}, 0.24 for Sr^{2+}, 0.26 for Co^{3+}, and 0.6 for O^{2-} in agreement with data reported in the literature for similar systems.[22,23] β was refined above 500 °C and increased monotonically with temperature. The maximum R_{wp} and R_p values for the refinements were respectively 25 and 15, but these relatively high values were due to problems with the refinement of the Pt reflections due to preferential orientation.

Results

Oxygen Deficiency. The oxygen stoichiometry of the powders at ambient temperature is illustrated in Figure 1. At ambient temperature $La_{1-x}Sr_xCoO_{3-\delta}$ is essentially stoichiometric ($\delta \approx 0$) up to about $x = 0.3$. For $x > 0.3$, the oxygen deficiency (δ) is increasing with increasing Sr content. The oxygen stoichiometry of Ca-substituted $LaCoO_3$ reported by Mastin et al.[2] and oxygen stoichiometry of $La_{1-x}Sr_xCoO_{3-\delta}$ at ambient temperature reported by Mineshige et al.,[4] Señaris-Rodríguez et al.,[24] and Lein et al.[6] are shown for comparison. The oxygen deficiency at elevated temperature, reported by Lankhorst et al.[25] and Lein et al.,[6] is also included in Figure 1 (800 and 900 °C). These data are in good agreement with the oxygen deficiency of $La_{1-x}Sr_xCoO_{3-\delta}$ first reported by Mizusaki et al.[26]

Crystal Structure at Ambient Temperature. The rhombohedral distortion from cubic perovskite structure, defined by the rhombohedral angle α, at ambient temperature was

(15) Petrov, A. N.; Kononchuk, O. F.; Andreev, A. V.; Cherepanov, V. A.; Kofstad, P. *Solid State Ionics* **1995**, *80* (3−4), 189−199.
(16) Caciuffo, R.; Rinaldi, D.; Barucca, G.; Mira, J.; Rivas, J.; Señaris-Rodríguez, M. A.; Radaelli, P. G.; Fiorani, D.; Goodenough, J. B. *Phys. Rev. B* **1999**, *59* (2), 1068−1078.
(17) Jiang, L. Z.; Xu, X. F.; Shen, J. Q.; Xu, Z. *J. Rare Earths* **2005**, *23*, 151−155.
(18) van Doorn, R. H. E.; Burggraaf, A. J. *Solid State Ionics* **2000**, *128* (1−4), 65−78.
(19) Wiik, K.; Andersen, Ø.; Grande, T.; Einarsrud, M.-A. Spray pyrolysis of complex oxide powders. In preparation.
(20) Rietveld, H. M. *J. Appl. Crystallogr.* **1969**, *2*, 65.
(21) Kirby, R. K. *Int. J. Thermophys.* **1991**, *12* (4), 679−685.
(22) Howard, C. J.; Kennedy, B. J. *J. Phys.: Condens. Matter* **1999**, *11* (16), 3229−3236.
(23) García-Muñoz, J. L.; Rodríguez-Carvajal, J.; Lacorre, P.; Torrance, J. B. *Phys. Rev. B* **1992**, *46* (8), 4414−4425.
(24) Señarís-Rodríguez, M. A.; Goodenough, J. B. *J. Solid State Chem.* **1995**, *118* (2), 323−336.
(25) Lankhorst, M. H. R.; Bouwmeester, H. J. M.; Verweij, H. *J. Solid State Chem.* **1997**, *133* (2), 555−567.
(26) Mizusaki, J.; Mima, Y.; Yamauichi, S.; Fueki, K.; Tagawa, H. *J. Solid State Chem.* **1989**, *80* (1), 102−111.

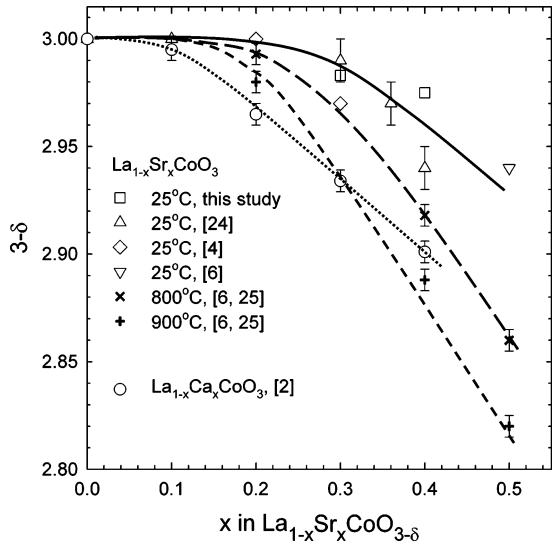

Figure 1. Oxygen nonstoichiometry as a function of x in $La_{1-x}Sr_xCoO_{3-\delta}$ at ambient temperature. Data from the literature for $La_{1-x}Sr_xCoO_{3-\delta}$ at ambient temperature,[4,5,24] 800 °C, and 900 °C[6,25] are included. Oxygen nonstoichiometry in $La_{1-x}Ca_xCoO_{3-\delta}$ at ambient temperature[2] is included for comparison. Lines are guides for the eyes. For some of the points the uncertainty is smaller than the size of the symbols.

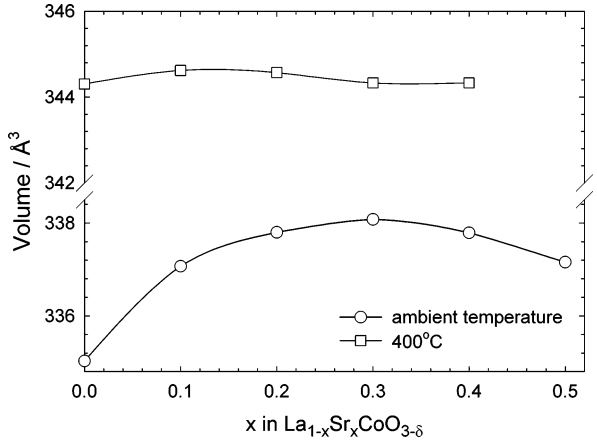

Figure 2. Unit-cell volume of $La_{1-x}Sr_xCoO_{3-\delta}$ as a function of the Sr content at ambient temperature and at 400 °C.

observed to decrease nearly linearly with composition predicting a transition to the cubic perovskite structure ($\alpha = 60°$) at the composition $La_{0.35}Sr_{0.65}CoO_{3-\delta}$. This is in good accordance with the data reported by Mineshige et al.[4] since the rhombohedral angle deviates from the linear dependence with composition at high Sr content. The unit-cell volume as a function of the Sr content in $La_{1-x}Sr_xCoO_{3-\delta}$ is shown in Figure 2. The unit-cell volume possesses a maximum at $La_{0.7}Sr_{0.3}CoO_{3-\delta}$ in accordance with a previous study.[18] At 400 °C (Figure 2), the unit-cell volume is almost independent of the Sr-substitution level.

Crystal Structure at Elevated Temperatures. The structure evolution of $La_{1-x}Sr_xCoO_{3-\delta}$ at elevated temperatures is depicted in Figure 3, where the evolution of the normalized lattice parameters $a/\sqrt{2}$ and $c/\sqrt{12}$ with increasing temperature is shown. The rhombohedral distortion, evidenced by the difference between $a/\sqrt{2}$ and $c/\sqrt{12}$, is clearly decreasing at ambient temperature with increasing Sr content. The a and c parameters are both affected by the Sr substitution. The deviation from the cubic symmetry is continuously decreasing by increasing the Sr content. Data

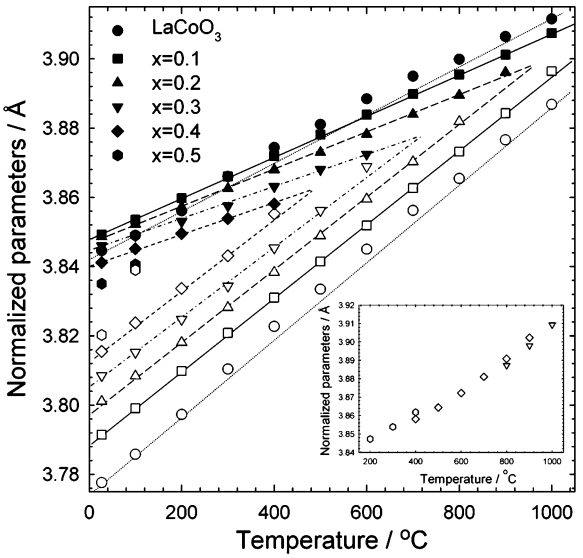

Figure 3. Normalized hexagonal lattice parameters of $La_{1-x}Sr_xCoO_{3-\delta}$ as a function of temperature. The lines are linear fits to the data. The inset shows the cubic lattice parameters for $x > 0.3$.

Table 1. Linear Thermal Expansion Coefficient (TEC) of *a* and *c* Lattice Parameters α_a and α_c for $La_{1-x}Sr_xCoO_{3-\delta}$ in Air and the Calculated Average Isotropic TEC, α_{iso}[a]

Sr content	linear thermal expansion coefficient (TEC)			temperature range/°C
	$\alpha_a/K^{-1} \times 10^5$	$\alpha_c/K^{-1} \times 10^5$	$\alpha_{iso}/K^{-1} \times 10^5$	
0.0	1.80	2.98	2.24	20−300; 1000
0.1	1.56	2.80	2.01	20−1000
0.2	1.28	2.71	1.85	20−1000
0.3	1.17	2.60	1.69	20−600
0.4	1.02	2.51	1.68	20−300
0.5	0.94	2.29		20−100

[a] The temperature range for each coefficient is given.

for $LaCoO_3$ reported by Mastin et al.[2] in a previous study are included. Thermal expansion of the two lattice parameters for $x \geq 0.1$ is linear over a wide range of temperature. Thermal expansion coefficients obtained by linear fit of the unit-cell parameters versus temperature are summarized in Table 1. The lattice parameter expansion coefficients of $LaCoO_3$ reported in Table 1 were calculated by linear fit to the lattice parameters below and above the magnetic transition, which induces the sigmoidal shape between 400 and 900 °C.[1,28,29] At high temperature, close to the phase transition, the c parameter deviates from the linear temperature dependence for $La_{0.7}Sr_{0.3}CoO_{3-\delta}$ and $La_{0.6}Sr_{0.4}CoO_{3-\delta}$. Above the transition temperature, the cubic lattice parameters possess a nonlinear dependency with temperature due to the onset of chemical expansion[5,6] caused by the loss of oxygen (Figure 1) and reduction of the valence of Co, see insert in Figure 3.

The compositional evolution of the TEC (thermal expansion coefficient) of the unit-cell parameters and isotropic thermal expansion of $La_{1-x}Sr_xCoO_{3-\delta}$ are shown in Figure 4. Corresponding data for $La_{1-x}Ca_xCoO_{3-\delta}$[2] are included for comparison. Thermal expansion of $La_{1-x}Sr_xCoO_{3-\delta}$ is con-

(27) Petrov, A. N.; Kononchuk, O. F.; Andreev, A. V.; Cherepanov, V. A.; Kofstad, P. *Solid State Ionics* **1995**, *80* (3−4), 189−199.
(28) Kriener, M.; Zobel, C.; Reichl, A.; Baier, J.; Cwik, M.; Berggold, K.; Kierspel, H.; Zabara, O.; Freimuth, A.; Lorenz, T. *Phys. Rev. B* **2004**, *69* (9), 094417.
(29) Gilbu, B.; Fjellvåg, H.; Kjekshus, A. *Acta Chem. Scand.* **1994**, *48* (1), 37−45.

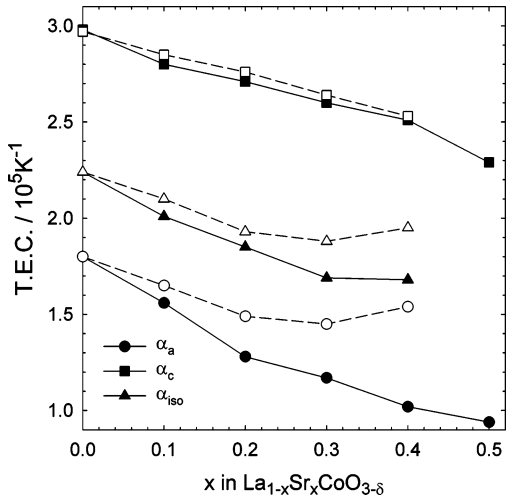

Figure 4. Linear thermal expansion coefficients of the lattice parameters, α_a and α_c, and isotropic volume expansion coefficient, α_{iso}, as a function of composition for $La_{1-x}Sr_xCoO_{3-\delta}$ (filled symbols). $La_{1-x}Ca_xCoO_{3-\delta}$ (open symbols) is shown for comparison.[2]

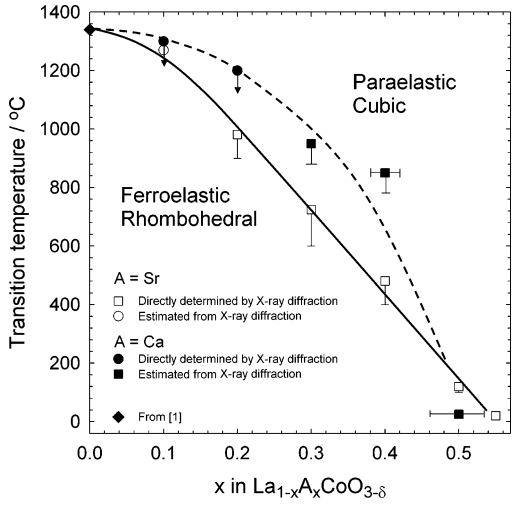

Figure 5. Phase diagram of $La_{1-x}Sr_xCoO_{3-\delta}$ showing the rhombohedral and cubic stability fields. Lines are guides for the eyes. Phase diagram for $La_{1-x}Ca_xCoO_{3-\delta}$ is shown for comparison.[2]

tinuously decreasing with increasing Sr content. While both systems present similar evolution of TEC for the *a* parameter, TEC for the *c* parameter and for the average linear thermal expansion are increasing at high Ca content for $La_{1-x}Ca_x$-$CoO_{3-\delta}$.

The rhombohedral to cubic phase transition temperature, T_c, was deduced from the HTXRD data. The transition temperature corresponds to the temperature where the reduced lattice parameters *a* and *c* become equal. T_c was preliminarily defined as the intercept of the linear fit of the reduced *a* and *c* unit-cell parameters. The evolution of T_c with the Sr content is shown in Figure 5. The transition temperature for pure $LaCoO_3$ has been reported at 1337 °C.[1] The phase transition could not be directly observed by X-ray diffraction for $La_{0.9}Sr_{0.1}CoO_{3-\delta}$ and T_c was estimated from the linear fit. This is an overestimation since the unit-cell parameters are expected to deviate from a linear relationship close to the transition, and this is illustrated in Figure 5 by the arrow pointing downward. For $x > 0.1$ in $La_{1-x}Sr_xCoO_{3-\delta}$, the phase transition could be observed by disappearance of the rhombohedral splitting of the X-ray reflections. For $x > 0.1$, T_c was estimated by the linear interpolation. The rhombohedral to cubic transition for $La_{0.45}Sr_{0.55}CoO_{3-\delta}$ at ambient temperature[4] is also included in Figure 5. The rhombohedral to cubic phase transition temperature in the $La_{1-x}Ca_xCoO_{3-\delta}$ system[2] is included in Figure 5 for comparison.

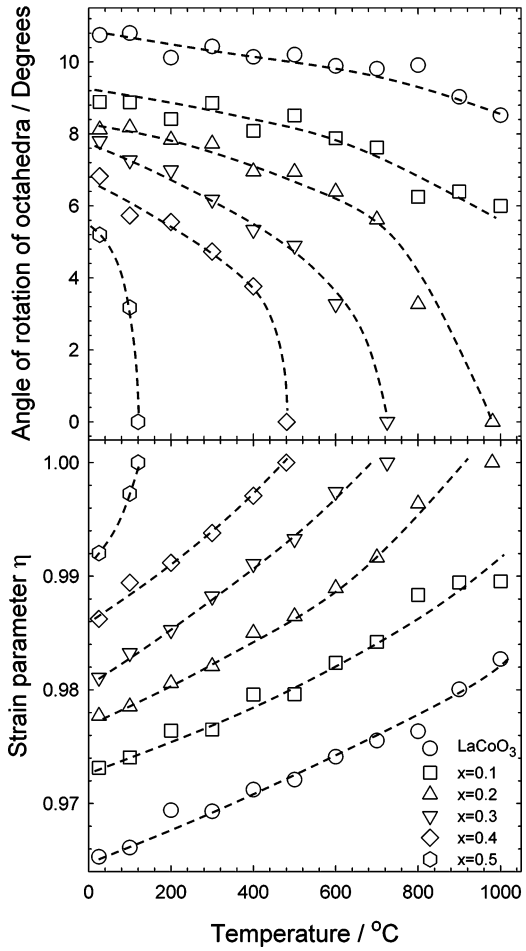

Figure 6. Angle of rotation of the CoO_6 octahedra and octahedral strain parameter as a function of temperature and composition. Lines are guides for the eyes.

Although X-rays are not very sensitive to Bragg scattering from oxygen, it was possible to refine the atomic displacement of oxygen from the HTXRD data. Refined oxygen coordinates for $LaCoO_3$ are slightly higher and are more scattered than those reported from neutron diffraction experiments, but they follow the same evolution with temperature as reported by Radaelli and Cheong[30] and Howard and coworkers[22,31] for similar materials. Octahedral angle of rotation around the 3-fold axis and the octahedral strain parameter for the different compositions can be estimated from the refined oxygen positions ($x = {}^1/_2 + u$). Equation 2 gives the angle of rotation, ϕ, of the octahedra in the rhombohedral perovskite:[22]

$$\tan \phi = 2u\sqrt{3} \qquad (2)$$

The evolution of ϕ as a function of temperature and composition is shown in Figure 6. At ambient temperature, the angle of rotation of the octahedra is decreasing with

(30) Radaelli, P. G.; Cheong, S. W. *Phys. Rev. B* **2002**, *66* (9), 094408.
(31) Howard, C. J.; Kennedy, B. J.; Chakoumakos, B. C. *J. Phys.: Condens. Matter* **2000**, *12* (4), 349−365.

increasing Sr content. At low temperature, for all substitution levels, the angle of rotation decreases almost linearly with temperature. Approaching the transition temperature, ϕ starts to deviate from the linear behavior and decreases rapidly toward zero. The onset temperature for the nonlinear behavior is decreasing with increasing Sr content.

In the rhombohedral structure with tilted octahedra, eq 3 gives the octahedral strain parameter, η:[22]

$$\eta = c \cos \phi / a\sqrt{6} \quad (3)$$

$\eta < 1$ means that the oxygen octahedra are compressed along the 3-fold axis and evolve to the regular cubic structure at high temperatures when it increases toward unity. Evolution of η with temperature for $La_{1-x}Sr_xCoO_{3-\delta}$ is included in Figure 6. $\eta < 1$ and increases continuously with increasing Sr content at ambient temperature. η is increasing almost linearly with temperature except close to the transition.

Discussion

Sr substitution in $LaCoO_3$ at ambient temperature is compensated mainly by oxidation of Co up to the composition $La_{0.7}Sr_{0.3}CoO_{3-\delta}$. At a higher level of Sr substitution the creation of oxygen vacancies becomes more energetically favorable compared to the stabilization of Co^{4+}, and the concentration of Co^{4+} saturates with increasing Sr content.[18,26] The difference in structural evolution of $LaCoO_3$ upon Sr or Ca substitution is caused by the difference in size of the two alkaline earth cations and the difference in the ability to stabilize Co in a high valence state. Substituting La^{3+} by Ca^{2+} results in a higher oxygen vacancy concentration in the materials compared to substitution by Sr^{2+} (Figure 1).[2] This difference is caused by the higher ability of SrO to stabilize the high oxidation state of Co relative to CaO. Creation of oxygen vacancies is also driving the rhombohedral structure toward the cubic perovskite structure. At elevated temperature, the increasing concentration of oxygen vacancies induces considerable chemical expansion of the $La_{1-x}Sr_xCoO_{3-\delta}$ materials with $x \geq 0.3$ [4,5] identified by the nonlinear thermal expansion of the lattice parameters (Figure 3).

At ambient temperature the lattice parameters evidenced a continuous evolution of the perovskite structure from the rhombohedral $R\bar{3}c$ phase for $LaCoO_3$, to the cubic $Pm\bar{3}m$ phase for $x > 0.55$. Because of the larger ionic radius[32] of Sr^{2+} (1.44 Å) compared to La^{3+} (1.36 Å), the Goldschmidt tolerance factor for the perovskite increases from 0.987 for $LaCoO_3$ to 1.015 for $La_{0.5}Sr_{0.5}CoO_{3-\delta}$. Here, we have assumed ideal perovskite structure, neglecting the influence of oxygen vacancies, and used the following ionic radii for Co:[32] Co^{4+} (0.53 Å high-spin state) and Co^{3+} (0.58 Å, average between the low-spin and the high-spin state due to the intermediate-spin state of Co as demonstrated by Asai et al.[33]).

The spin state of Co in $La_{1-x}Sr_xCoO_{3-\delta}$ is still a subject of controversy.[16,28,34] In $LaCoO_3$, the thermally induced magnetic transition from intermediate spin to high spin is evidenced by the sigmoidal shape of the lattice parameter evolution with temperature[30] and by the higher thermal expansion coefficient compared to other $LaMO_3$ (M = Fe,[35] Cr,[29] Mn,[36] and Ni).[37] With substitution of La^{3+} by Sr^{2+}, Co^{4+} is introduced which stabilizes the intermediate-spin state of Co^{3+} in its vicinity.[34] The influence of magnetic transition on the thermal expansion could not be detected for the substituted materials, except that TEC is strongly reduced with increasing substitution level; see Figure 4.

The increase of the unit-cell volume for $x < 0.3$ shown in Figure 2 reflects the larger radius difference between La^{3+} and Sr^{2+} compared to the difference between Co^{3+} in the intermediate-spin state and Co^{4+}. The reduction of the unit cell for $x > 0.3$ is not expected since the Sr substitution becomes gradually more compensated by oxygen vacancies in this region. Van Doorn et al. reported similar evolution of the unit-cell volume as a function of the Sr content up to $x = 0.7$.[18] They reported microdomains with a tetragonal $a_c * a_c * 2a_c$ superstructure in $La_{0.3}Sr_{0.7}CoO_{3-\delta}$ due to the ordering of oxygen vacancies. Similar domains have also been reported for $La_{0.6}Sr_{0.4}CoO_{3-\delta}$ by Kruidhof et al.[38] Ordering of oxygen vacancies is however expected to increase the unit-cell volume in contradiction to the experimental findings (Figure 2). At high temperature, the volume of the unit cell is less dependent on the Sr concentration (Figure 2). Finally, it is also important to note that the significant variation of the TEC with Sr substitution (Table 1) is affecting the dependence of how the isothermal volume changes with Sr-substitution level.

The thermal expansion of *a* and *c* unit-cell parameters of $La_{1-x}Sr_xCoO_{3-\delta}$ is decreasing almost linearly with the Sr content (Figure 4), while the corresponding data for $La_{1-x}Ca_xCoO_{3-\delta}$ show that thermal expansion possesses a minimum with increasing Ca content. Mastin et al.[2] discussed the influence of the oxygen vacancy concentration on the thermal expansion. The difference of the thermal expansion coefficients in the two systems can be attributed to the considerably lower vacancy concentration in $La_{1-x}Sr_xCoO_{3-\delta}$ compared to $La_{1-x}Ca_xCoO_{3-\delta}$.[2] In $La_{1-x}Sr_xCoO_{3-\delta}$ the thermal expansion is mainly affected by the substitution of La^{3+} by Sr^{2+}, stabilizing the IS state of Co^{3+}. The more pronounced effect of oxygen vacancy concentration on the *a* unit-cell parameter can possibly be related to a vacancy-ordering mechanism.[2]

The dependence of the angle of rotation of CoO_6 octahedra with Sr content and temperature is presented in Figure 6. The temperature dependence is essentially similar to the

(32) Shannon, R. D. *Acta Crystallogr.* **1976**, *A32*, 751−767.
(33) Asai, K.; Yoneda, A.; Yokokura, O.; Tranquada, J. M.; Shirane, G. *J. Phys. Soc. Jpn.* **1998**, *67* (1), 290−296.
(34) Muta, K.; Kobayashi, Y.; Asai, K. *J. Phys. Soc. Jpn.* **2002**, *71* (11), 2784−2791.
(35) Fossdal, A.; Menon, M.; Waernhus, I.; Wiik, K.; Einarsrud, M.-A.; Grande, T. *J. Am. Ceram. Soc.* **2004**, *87* (10), 1952−1958.
(36) Hammouche, A.; Siebert, E.; Hammou, A. *Mater. Res. Bull.* **1989**, *24* (3), 367−380.
(37) Obayashi, H.; Kudo, T. *Jpn J. Appl. Phys., Part 2* **1975**, *14* (3), 330−335.
(38) Kruidhof, H.; Bouwmeester, H. J. M.; Vondoorn, R. H. E.; Burggraaf, A. J. *Solid State Ionics* **1993**, (63−65), 816−822.

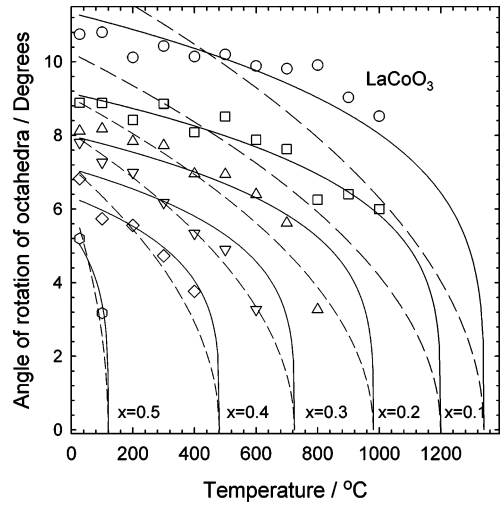

Figure 7. Angle of rotation of $La_{1-x}Sr_xCoO_{3-\delta}$ with the numerical fit for a second-order phase transition (dotted line) and a tricritical phase transition (bold line).

Table 2. Constant A for $La_{1-x}Sr_xCoO_{3-\delta}$ Determined by Fitting the Order Parameter, ϕ, to the Equation $\phi = A(T - T_c)^n$ for a Second Order ($n = 1/2$) and a Tricritical ($n = 1/4$) Phase Transition

		A	
Sr content	T_c (°C)	$n = 1/2$	$n = 1/4$
0	1340	0.34	1.87
0.1	1200	0.30	1.55
0.2	980	0.29	1.43
0.3	720	0.30	1.37
0.4	450	0.32	1.35
0.5	120	0.57	1.61

behavior of rhombohedral rare-earth aluminates[31] and $La_{1-x}Ca_xCoO_{3-\delta}$.[2] The angle of rotation is increasing with the Ca content in $La_{1-x}Ca_xCoO_{3-\delta}$ for $x > 0.1$, while the strain parameter remains constant. This is due to the increasing oxygen vacancy concentration for these materials.[2]

The angle of rotation, ϕ, is a suitable order parameter for the phase transition.[2,31] Howard and Stokes[41] have discussed the nature of the phase transition in rhombohedral perovskites like $LaAlO_3$ or $PrAlO_3$[39] using a mean field theory treatment of the phase transition. The temperature variation of the angle of rotation for $La_{1-x}Sr_xCoO_{3-\delta}$ can be fitted to an expression of the type $A(T - T_c)^n$ where n is either $1/2$ or $1/4$ corresponding respectively to a second order or a tricritical phase transition[31] and A is a material-dependent constant. Figure 7 shows how these two models fitted to the experimental data. The parameters obtained by the fit are summarized in Table 2. The tricritical phase transition model provides better agreement with the evolution of the angle of rotation of the octahedra. A similar study of the angle of rotation in $La_{1-x}Pr_xAlO_3$ by Kennedy and co-workers[39] has demonstrated a possible change of the nature of the phase transition by chemical substitution. Indeed, the phase transition in $LaAlO_3$ is a second-order phase transition while $PrAlO_3$ seems to display an apparent tricritical phase transition.[39] However, the nature of this tricritical phase transition is still a subject of debate.[39,41,42] The mean field theory was also applied to the data reported for $La_{1-x}Ca_xCoO_{3-\delta}$.[2] For $x = 0.1$, a tricritical model with $A = 1.54$ gives a good description of the experimental data. The value of A is then comparable with $La_{1-x}Sr_xCoO_{3-\delta}$ for $x = 0.1$. However, for $La_{1-x}Ca_xCoO_{3-\delta}$ with $x > 0.1$, it was not possible to apply the crystallographic data due to significant influence of the oxygen vacancy concentration on the order parameter, which is not accounted for in the mean field theory. Finally, the nature of the phase transition can also alternatively be analyzed by the spontaneous strain,[41] calculated from the lattice parameters above and below the transition temperature. However, due to the extensive chemical expansion in the cubic state, the spontaneous strain of Sr- and Ca-substituted $LaCoO_3$ is not possible to estimate.

The crystal structure and the rhombohedral to cubic phase transition temperature are important for the understanding of the ferroelastic properties of Sr- and Ca-substituted $LaCoO_3$. Most important for the mechanical properties is the possibility for domain reorientation under mechanical load, and here the thickness and energy of the domain walls are of particular importance.[12] The thickness of the domain walls, w, separating ferroelastic domains, is temperature-dependent and can be described by

$$w \propto 1/(T_c - T) \tag{4}$$

According to the Landau-Ginzburgh theory,[12] the velocity of the domain wall is related to the energy of the domain wall, E_{wall}, which is dependent on the phase transition temperature:

$$E_{wall} \propto (T - T_c)^{3/2} \tag{5}$$

When the Ca or Sr content is increased, the rhombohedral to cubic phase transition temperature is depressed (see Figure 5), which will result in a lower E_{wall} and consequently a decrease of the cohersive stress. The different evolution of the rhombohedral to cubic phase transition temperature for the $La_{1-x}Sr_xCoO_{3-\delta}$ and $La_{1-x}Ca_xCoO_{3-\delta}$ systems may also cause a difference in the ferroelastic behavior of the materials. Therefore, by controlling the substitution level of alkaline earth in $LaCoO_3$-based materials, it may be possible to tailor the ferroelasticity and thereby the mechanical properties of the materials and this will be followed up in future studies. By investigating coupling of ferroelasticity with functional properties, it could be possible to develop devices with multiferroic properties.

Conclusion

Sr-substituted $LaCoO_3$ has been shown to be a rhombohedral perovskite up to about 55 mol % Sr. The rhombohedral to cubic phase transition temperature and thermal expansion of $La_{1-x}Sr_xCoO_{3-\delta}$ have been determined as a function ofSr content by high-temperature X-ray diffraction.

(39) Carpenter, M. A.; Howard, C. J.; Kennedy, B. J.; Knight, K. S. *Phys. Rev. B* **2005**, *72* (2), 024118.
(40) Kennedy, B. J.; Howard, C. J.; Prodjosantoso, A. K.; Chakoumakos, B. C. *Appl. Phys. A* **2002**, *74*, 1660−1663.
(41) Howard, C. J.; Stokes, H. T. *Acta Crystallogr. A* **2005**, *61*, 93−111.
(42) Salje, E. K. H.; Hayward, S. A.; Lee, W. T. *Acta Crystallogr. A* **2005**, *61*, 3−18.

The phase diagram of the $La_{1-x}Sr_xCoO_{3-\delta}$ system has been determined, displaying the stability field of the rhombohedral and cubic perovskite phase. The order parameter of the rhombohedral to cubic phase transition has been shown to be related to the angle of rotation of the CoO_6 octahedra, which also correspond to the ferroleastic order parameter in these materials. Finally, the difference between the properties of Sr and Ca substituted $LaCoO_3$ has been pointed out.

Acknowledgment. Financial support from the Research Council of Norway is acknowledged.

CM061539K